Main Group Chemistry
Vol. 7, No. 3, September 2008, 205–215

Taylor & Francis
Taylor & Francis Group

Mercury adsorption on PdAu, PdAg and PdCu alloys

Shela Aboud, Erdem Sasmaz and Jennifer Wilcox*

Department of Energy Resources Engineering, Stanford University, Stanford, California, USA

(*Received 3 July 2008*)

Under specific conditions, sorbent materials such as activated carbon, metal oxides, metal sulfides and pure metals can effectively capture mercury (Hg). Among these materials activated carbon is one of the most widely-used sorbents because of its high removal capacity. Unfortunately, activated carbon can hinder the recycling of particulate matter for concrete manufacturing because it prevents concrete from meeting the freeze-thaw requirements. The use of a sorbent material that can capture Hg efficiently but is also concrete-friendly would allow for the increased sale of waste materials, ultimately oversetting landfill costs. In this work, density functional theory calculations have been used to predict the binding mechanism of Hg on the binary alloys PdAu(111), PdAg(111), PdCu(111) which are potential candidates for concrete-friendly sorbents. Although bulk Pd surfaces are more reactive than bare Au, Ag and Cu surfaces, the addition of small amounts of Au, Ag and Cu alloyed with the Pd acts to increase the overall mercury binding energy. Interestingly, it has been found that the dopant atoms in the PdAu, PdAg and PdCu alloys increase the Hg adsorption most effectively when they remain in sub-surface layers.

Keywords: mercury; Hg; PdAu; PdAg; PdCu; alloys; density function theory; binding energy

Introduction

Coal combustion is responsible for 25% of the world's energy use [1], and recent projections show that its use is expected to rise 2.5% over the next 10 years [2]. With the increasing demand on coal, removing hazardous materials from combustion fuel gases has become an important issue. The United States Environmental Protection Agency (USEPA) adopted the Clean Air Mercury Rule to reduce the release of mercury (Hg) from coal-fired power plants ultimately curbing US Hg emissions by 70% [3]. Although this rule was vacated by congress in February 2008, roughly half of the states still have Hg emissions controls in place for coal-fired power utilities.

There are various sorbent materials, including activated carbon, metal oxides, metal sulfides and pure metals that can adsorb elemental Hg [4,5]. Among these materials, activated carbon is one of the most widely used and halogenated and sulfur-impregnated activated carbon are highly efficient sorbents [6–10]. Mercury binding on halogenated activated carbon has also been investigated theoretically, showing higher energies compared to virgin activated carbon [10]. Despite the ability of activated carbon to effectively remove Hg it can be expensive due to the high cost of raw materials,

*Corresponding author. Email: jen.wilcox@stanford.edu

ISSN 1024-1221 print/ISSN 1745-1167 online

DOI: 10.1080/10241220802465213
http://www.informaworld.com

particularly because it cannot be reused. Furthermore, activated carbon can degrade fly ash, a coal combustion byproduct that can be used for asphalt or concrete manufacturing, minimizing potential landfill materials. Within the concrete manufacturing process the addition of spent activated carbon prevents concrete from meeting the freeze-thaw requirements, jeopardizing its functionality [11]. Additionally, preventing Hg release from coal gasification will require a sorbent that can withstand elevated temperatures. Activated carbon fails to meet this requirement because it breaks down at approximately 130°C [12]. The Pd-based sorbents examined in this work can withstand temperatures up to approximately 400°C making them attractive for high-temperature gasification applications [13]. The goal of this work is to use density functional theory (DFT) to investigate potentially thermally stable, concrete-friendly sorbent materials that still retain a high Hg removal capacity and can be reused, making it more affordable and environmentally benign.

Transition metal sorbents have been proposed for efficiently adsorbing semi-volatile elements such as Hg [13–15]. In general, they are attractive because they can be regenerated. Because they can be used at high temperatures, the impact on combustion byproducts is reduced since waste materials can then be removed upstream. In particular, Pd has been shown to have a strong propensity for adsorbing Hg at high temperature [14] and in fact, it is interesting to note that Pd has even been used to recover Hg vapour emissions from dental amalgams [16]. One serious issue with employing pure Pd sorbents in the combustion environment of the flue gas is its high susceptibility to sulfur (S) poisoning. To reduce the adsorption of S in hydrogen separation membranes, Pd doped with noble metals such as Au, Cu and Ag have been proposed and these alloyed materials demonstrate a higher S tolerance [17]. In this work, DFT is used to investigate the adsorption of Hg on PdM (111) (M = Au, Ag, Cu) alloyed surfaces as a function of total and surface M composition to determine whether these alloy materials will also show a high Hg binding. To the authors knowledge this group's work represents the first study of Hg adsorption on alloyed transition metal surfaces. A density of states analysis is conducted to examine the nature of the electronic interactions between the Hg and the alloy surfaces to correlate the strength of the interaction with the primary binding mechanisms. A detailed understanding of these mechanisms will provide insight that can be used to engineer these high temperature sorbent materials for more efficient Hg capture.

Computational details

DFT calculations have been performed using the Vienna *ab initio* Simulation Package (VASP) [18]. Ultrasoft Vanderbilt pseudopotentials are used to describe core orbitals [19] and electron exchange correlation functionals were calculated using the Perdew and Wang [20] approximation described by a generalized gradient approximation (GGA). Although DFT calculations generally give reliable results for metal atoms, for heavy elements such as Hg, both relativistic and correlation effects must be included for adequate geometry and energy predictions [21]. To validate the accuracy of the pseudopotentials, the bond length (r), dissociation energy (D_e) and harmonic vibrational frequency (ω_e) of an Hg_2 dimer have been calculated and compared against experimental data; the results are given in Table 1. For these test calculations, a plane-wave expansion with a cutoff of 350 eV was employed for Hg and the residual minimization method for relaxation was performed with a single k-point. As can be seen from Table 1, the vibrational frequency calculated for the Hg_2 dimer is in good agreement with experiment [22] deviating by two wavenumbers.

Table 1. Spectroscopic parameters for Hg_2 dimer.

Parameter	Hg_2 dimer	
	DFT	Exp[a]
Bond length (Å)	3.61	3.69
Dissociation energy (kcal/mol)	1.16	1.09
Vibrational frequency (cm^{-1})	21.8	19.7

[a]Ref. [23].

For the surfaces simulations, a plane-wave expansion with a cutoff of 350 eV was used and to relax the atoms in the structure, a Methfessel and Paxton [23] Gaussian-smearing of order 1 was used with a width of 0.05 eV, maintaining a difference of 1 meV/atom between the calculated free energy and total energy. Geometric relaxation was obtained with the conjugate-gradient (CG) algorithm until the forces on all the unconstrained atoms were less than 0.03 eV/Å. Calculations of PdM alloys are run with p(2 × 2) surface cells for a total of four metal atoms per layer using both two- and four-layer slabs. The surface Brillouin zone integration is calculated with a 7 × 7 × 1 Monkhorst-Pack [24] k-point mesh and each slab is separated by a 10 Å-thick vacuum region to prevent interactions between neighbouring slabs. To represent the Hg-adsorbed structure a single adatom was placed on the surface corresponding to a coverage of $\theta = 0.25$ ML. Because of the excessive number of spatial permutations of Pd and M atoms in a four-layer slab, as an initial study the positions of the M atoms in the various layers are chosen at random and the binding energy of Hg is calculated as a function of the total M% composition. By restricting the simulation domain to two-layer slabs the precise surface-to-total concentration ratio of Pd can be examined and the correlation between the binding energy of Hg and the position of Pd and M atoms can be further determined.

Results and discussion

Pd alloy lattice constants

The equilibrium lattice constants of the Pd, Au, Ag, Cu and the Pd binary alloys are first calculated and shown in Figure 1, where a 0% M composition corresponds to pure Pd, and a 100% M composition corresponds to pure M. As can be seen the simulated lattice constants are close to the experimental values [25] with an error of approximately 1.1–2.5%. The lattice constants are compared against Vegard's law using Equation (1),

$$\alpha_{PdM} = \alpha_M \chi_M + (1 - \chi_M)\alpha_{Pd} \quad (1)$$

where α_{PdM}, α_{Pd}, α_M and χ_M refer to the lattice constant of the PdM alloy at the desired composition, the lattice constant of pure Pd, the lattice constant of pure M and the mole fraction of M of the alloy, respectively. The application of Vegard's law to the calculated lattice constants of pure Pd and M yielded comparable alloy lattice constants to the DFT calculations. The PdAg and PdAu alloy lattice spacing increases as a function of increasing Au and Ag composition and the reverse trend is observed for PdCu consistent with the relative lattice constants of pure Ag, Au and Cu with respect to Pd.

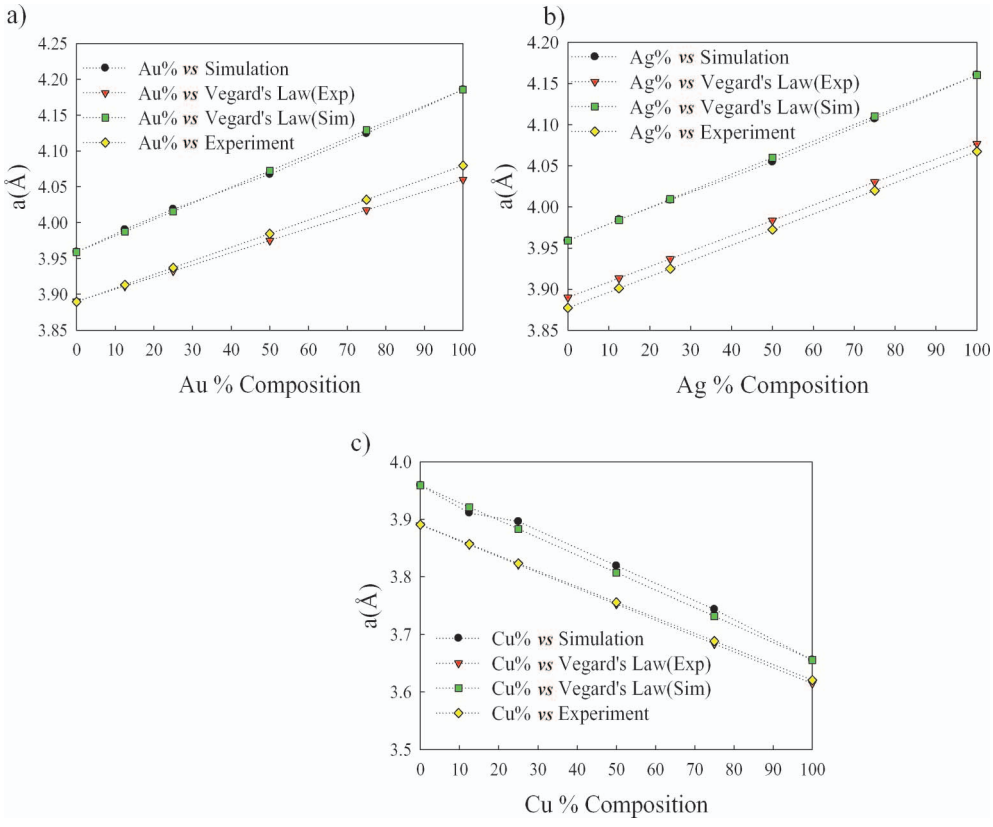

Figure 1. Effect of M% composition on the lattice constant of PdM(111).

Binding energy

The PdM(111) surface has been modelled as an ordered fcc crystal structure and the adsorption of Hg has been examined on the top, bridge, pure and mixed three-fold adsorption sites. The binding energy, E_{bind}, on each surface site was calculated using Equation (2),

$$E_{\text{bind}} = E_{\text{complex}} - [E_{\text{adatom}} + E_{\text{surface}}] \tag{2}$$

where E_{complex}, E_{adatom} and E_{surface} represent the total energies of the adsorbate substrate complex, the adsorbate adatom and substrate surface, respectively. The top and bridge sites of pure Pd(111), Au(111), Ag(111) and Cu(111) surfaces are found to be unstable and the fcc and hcp sites are the most reactive to Hg. Calculated binding energies of Hg on fcc and hcp sites are −22.01 kcal/mol, −22.25 kcal/mol on Pd(111), −10.08 kcal/mol, −10.1 kcal/mol on Au(111), −8.49 kcal/mol, −8.56 kcal/mol on Ag(111) and −14.92 kcal/mol, 15.07 kcal/mol on Cu(111), respectively. In this initial study, the positions of the M atoms in the various layers of the four-layer slab simulations are chosen at random because of the large number of spatial permutations of the Pd and M atoms; therefore, the binding energy of Hg is calculated as a function of the total M% composition. Calculations using these four-layer slabs of PdAu(111) show that the binding

energy of Hg is sensitive to the number of Pd and Au atoms surrounding the adsorption sites. As shown in Figure 2, increasing the %Au composition can increase the binding energy of Hg but it also can increases the probability of creating a configuration of atoms that has a lower binding energy. This suggests that the binding energy of Hg is dependent on the physical position of Au and Pd atoms rather than just the total percentage of Au inside the alloy.

To further investigate the correlation between the binding energy and the physical position of the dopants in the alloyed materials, simulations of Hg on PdM(111) surfaces are run using two-layer slab structures to control the total M% composition and surface M% composition independently. Calculated binding energies on the PdM(111) alloys at hcp sites are illustrated in Figure 3. In general, it can be seen that the binding energies of Hg on PdM(111) lie between the binding energies of Hg on pure Pd(111) and M(111) for both hcp sites. However, higher binding energies have been obtained at 12.5% and 25% total M compositions when the surface M% composition is 0% and 25%.

It is expected that in each of the alloyed materials there will be an optimal M% composition that maximizes the binding energy. In fact, from the figures it can be concluded that the addition of a small amount of M = Au, Ag and Cu, i.e., 12.5–25%, increases the binding energy of Hg on the PdM(111) surface, whereas higher levels of M composition decreases the binding energy. However, in some cases, it has been found that the binding energy depends not only on the total M% composition but also on the specific location of the Pd, Au, Ag and Cu atoms relative to the binding site and a lower binding energy has been observed even at low total M% composition and M% surface composition for both fcc and hcp adsorption sites. This behavior appears to be due to the ability of the Au, Ag and Cu atoms to increase the surface reactivity when located in the sub-surface layers by enhancing the surface Pd atoms capacity to bind the Hg. Specifically, the two factors that affect the binding energy of Hg on PdM(111) at the same total and surface M% compositions are the number of Pd atoms surrounding the adsorption site on the top layer and the number of neighbouring Au, Ag and Cu atoms in the bottom layer. This observation was also confirmed through an additional calculation carried out at 12.5% total and 0% surface Au composition at a pure hcp site. The binding energy at an hcp site with the Au atom at the bottom is 2 kcal/mol higher than the site

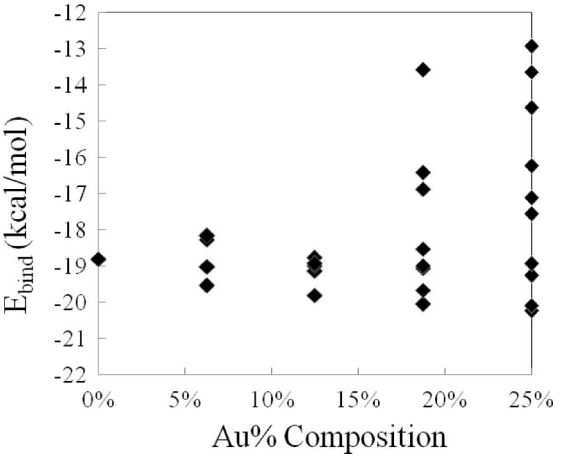

Figure 2. Mercury adsorption energy as a function of Au composition in PdAu alloy.

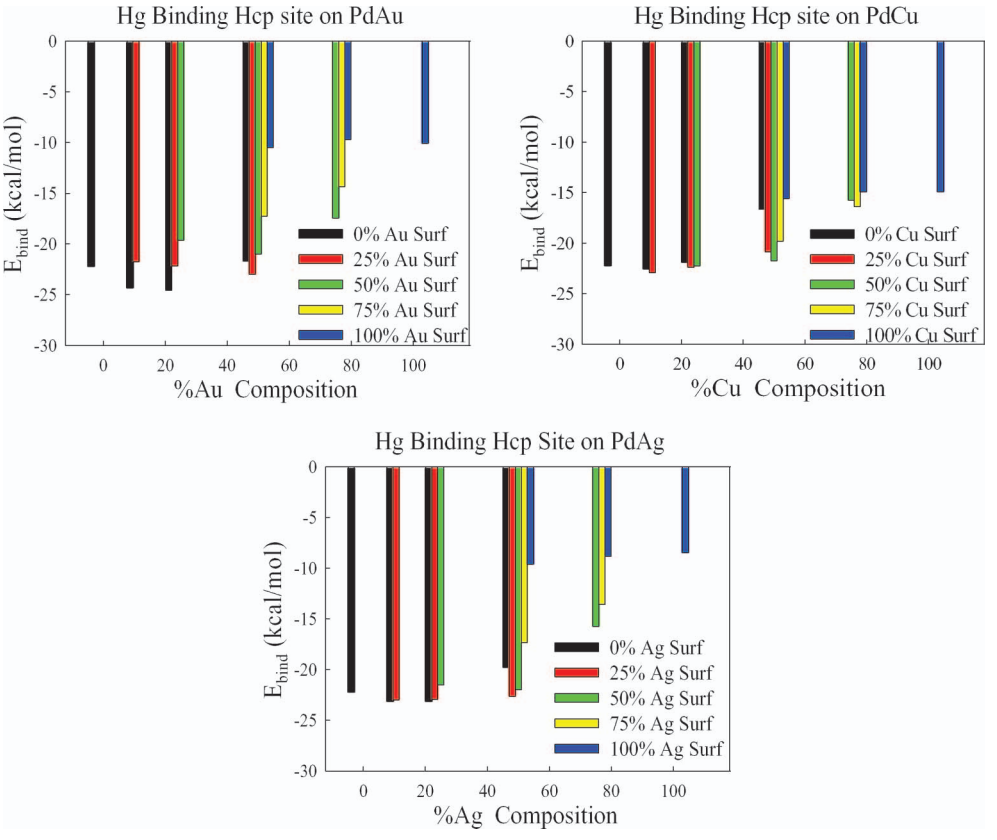

Figure 3. Binding energy of Hg on three-fold hcp site on PdM (111) binary alloys.

with the Pd atom lying below the Hg atom. Furthermore, it has been observed that pure Pd three-fold surface adsorption sites are more stable than mixed sites and in mixed sites the Hg prefers to stay closer to the Pd atoms than the Au, Ag and Cu atoms. Because in all cases the maximum Hg binding corresponds to the three-fold site for the (111) alloys suggests that improved reactivity could result at the four-fold adsorption sites that occur for (100) surfaces. In fact recent DFT calculations of Hg adsorption on pure transition metals have found this to be the case [15]. In the present work, the (111) surface was investigated because it is more energetically stable than the (100) surface.

Density of states

The Pd alloy simulation results suggest that the binding energy of Hg is dependent on the physical position of the M and Pd atoms rather than just the total percentage of M inside the alloy. To understand the impact of the alloying material on the electronic structure due to Hg adsorption, comparisons were made between the three types of alloy materials for a precise atomic configuration of 18.75% M corresponding to a relatively high Hg binding energy. The local density of states (LDOS) of the individual atoms and the specific *s*-, *p*- and *d*-states is calculated by projecting the wave functions from the DFT onto spherical harmonics centered at each of the atomic sites. On the left side of Figure 4 are plots of the

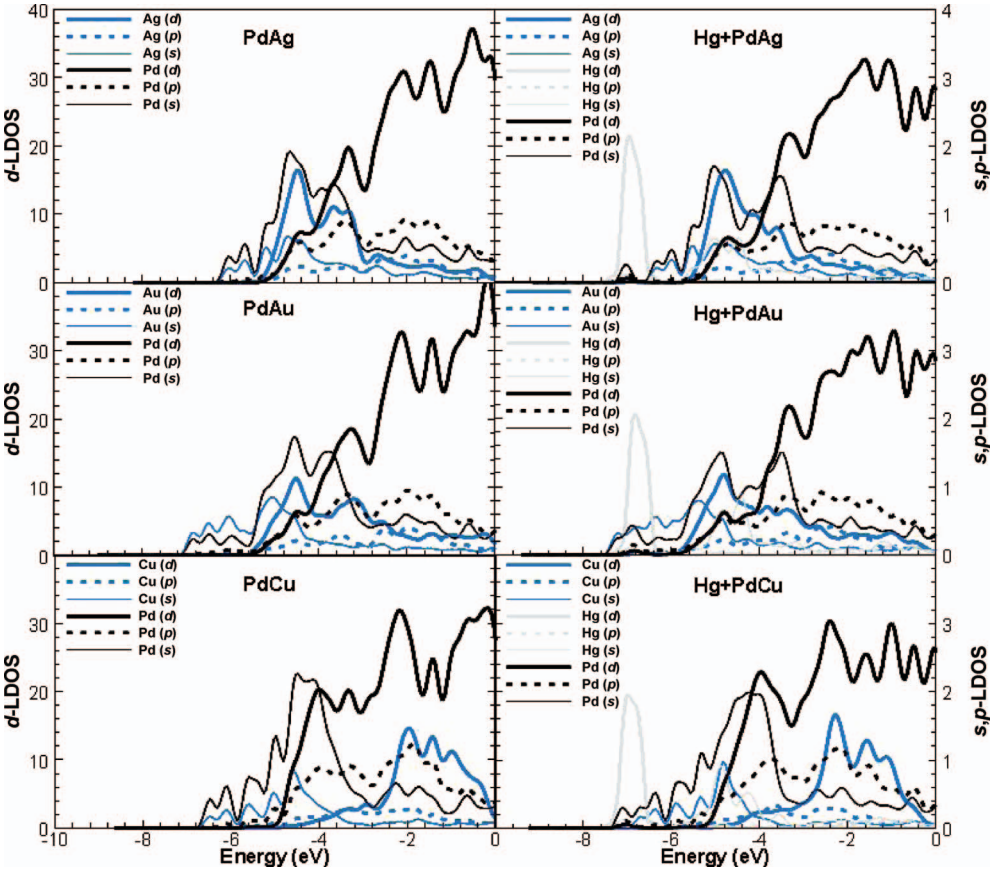

Figure 4. LDOS for *s*-, *p*- and *d*-states of atoms in PdM alloys before and after Hg adsorption.

LDOS for the clean PdM alloys and on the right side are plots of the LDOS after Hg is adsorbed onto the PdM surface, only the states below the Fermi level located at 0 eV are shown. One feature that is evident in the plots is the strong overlap of the Hg *d*-band with the *s*- and *p*-band of Pd at around 7 eV. In the PdAu and PdCu the *s*-states of the Pd and dopant extend to lower energies prior to Hg adsorption resulting in a modification of the shape of the states, whereas for PdAg a new resonance peak occurs at the Hg *d*-band energy. Although the Hg capture induces a resonance in the Pd states, there is little effect from the M states. Even states that are initially in the vicinity of the Hg *d*-band are only slightly modified. This supports the idea that the Hg-Pd interaction is the dominant mechanism, and the dopant M only acts to modify this interaction. In addition, calculations of the *d*-band center of the Pd, the dopant M and the combined PdM are shown in Table 1 for each of the alloyed systems. The trend in the Pd *d*-band center in the alloyed materials is a shift to the right for the alloys with higher adsorption energies. In contrast, the *d*-band centers of the dopants M as well as the average *d*-band centre of the total PdM alloy both show a shift to the left for the alloys with higher binding. Again, it should be stressed that these results only correspond to a single alloy composition in a single configuration and further tests should be made to determine how much the observed behavior is dependent on structure.

A comparison of the LDOS is shown in Figure 5 for Hg in the gas phase and Hg adsorbed to the alloy surfaces, where the Fermi level located at 0 eV. The *d*-band of Hg is shifted to lower in energies as it adsorbs to the surface and both the *s*- and *p*-states are significantly broadened after adsorption all of which signifies a strong interaction with the surface. Furthermore, the *p*-state after adsorption extends below the Fermi level which denotes the filling of the *p*-orbitals in the adsorbed Hg. The integral of the LDOS up to Fermi level is proportional to the number of electrons and for the *p*-band of Hg after adsorption on PdAg, PdAu and PdCu corresponds to 1.73, 1.59 and 1.62 electrons, respectively. Consistent with the change in electron density of the Hg atom the work functions of all three alloys decreases as shown in Table 2. The work function is calculated as the difference in energy between the potential in the vacuum region and the Fermi level.

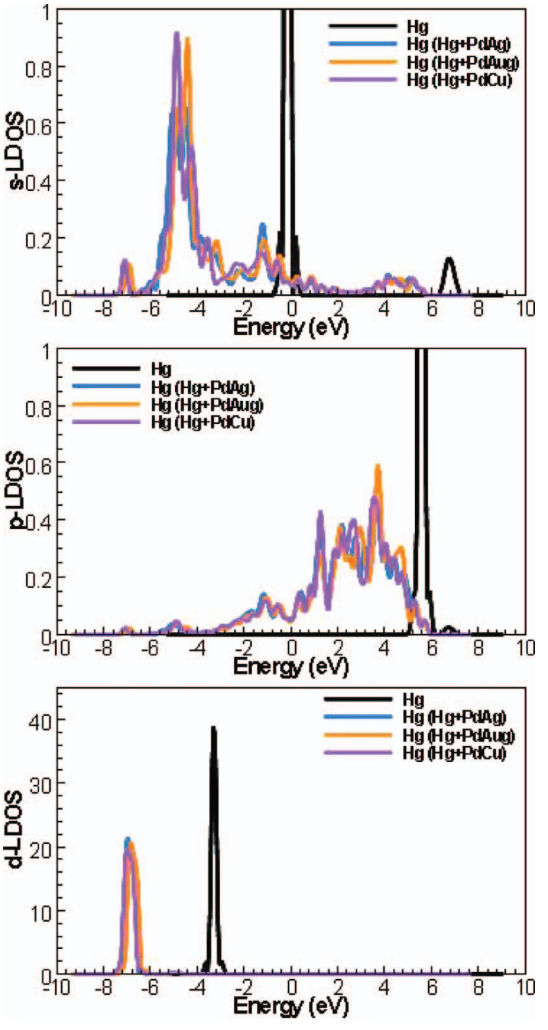

Figure 5. LDOS of Hg in the gas phase compared to Hg bound to the surface of the PdAg, PdAu and PdCu alloys. The top, middle and bottom pictures correspond to the *s*-states, *p*-states and *d*-states, respectively.

In general, the change in work function can be attributed to a change in the surface dipole caused by two competing mechanisms; a spreading out of the surface charge and Smoluchowski smoothing [26]. The first results in a negative dipole layer which increases the work function while the smoothing acts to reduce the work function. To examine the surface dipole layer, the change in charge density is averaged along the direction perpendicular to the surface. The change in charge density is defined by Equation (3),

$$\Delta\rho(z) = \rho_{\text{tot}}(z) - \rho_{\text{surf}}(z) - \rho_{\text{ads}}(z) \tag{3}$$

where the first term is the total charge density, the second term is the charge density of just the surface and the third term is the charge density of just the Hg atom. The result for the PdAu alloy is shown in Figure 6, where the position of the surface layers (blue circles; see Graphics Abstract and online version) and the Hg (grey circle) is superimposed over the plot. A negative charge density corresponds to an accumulation of electrons and as can be seen there is an increase in electron density around the Hg and a decrease in electron density between the Hg and the surface. The net result is positive surface dipole which is consistent with the calculated decrease in the work function after adsorption. Finally, the change in work function upon Hg adsorption is also calculated for pure Pd, also shown in Table 2,

Table 2. Binding energy, workfunction and *d*-band centre for Pd and PdM alloys.

				d-Band centre (eV)		
	E_{bind} (eV)	Φ(eV)	ΔΦ(eV)	Pd	M	PdM
Pd	0.839	5.336	−1.527	−1.650	–	–
PdAg	0.903	5.040	−1.484	−1.478	−3.351	−1.839
PdAu	0.886	5.404	−1.697	−1.466	−2.964	−1.747
PdCu	0.840	5.113	−1.616	−1.674	−1.528	−1.646

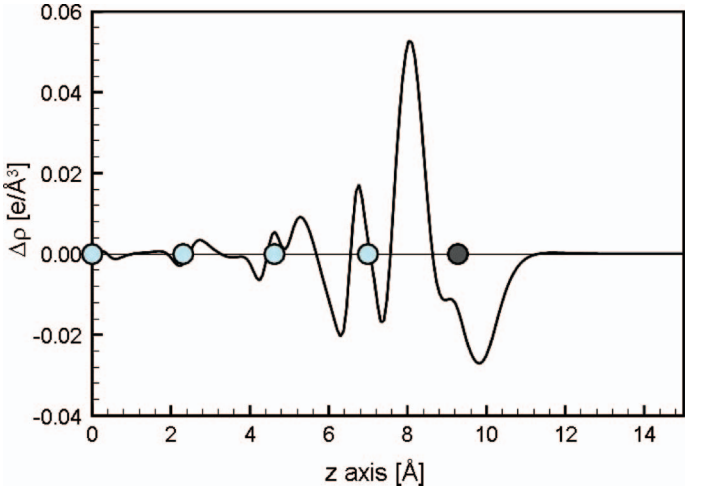

Figure 6. Average charge density change after the adsorption of Hg on a PdAu surface along the direction normal to the surface. Negative charge density corresponds to an accumulation of electrons.

and is higher than in other DFT studies of Hg capture on Pd [15] and can be attributed to the use of a different nonlocal correction [26].

Summary

The Hg binding on two-layer slabs of PdM(111) (M = Ag, Au and Cu) has been studied as a function of total and surface M% compositions and lower binding energies have been obtained as the total M% composition increases. The binding energy of Hg is found to be strictly dependent on the position of the M and Pd atoms located at the surface and sub-surface layers rather than total percentage of M inside the alloy. However, on four-layer slabs small additions of M can increase or decrease the PdM(111) surface reactivity for elemental Hg depending on the local configuration of atoms. A LDOS analysis at a concentration of 18.75% was performed to investigate the interaction between the Hg and the PdM alloys for a high binding composition. The binding was primarily found to stem from the *d*-band of the Hg interacting with the *s*-, *p*- and *d*-bands of the Pd atoms. This is consistent with the trend in the Pd *d*-band centre for the alloyed materials, which shifts to the left for higher adsorption energies. In addition, it is found that the work function decreases after Hg adsorption for each of the Pd alloys studied resulting from the decrease in the electron density at the surface as the Pd alloy removes electrons from the Hg. Further work needs to be done to elucidate whether the binding mechanisms found in this study are reflective of the alloys in general or just the local composition for the specific example.

References

[1] J.M.D. Tascon, Recent Developments in the International Scenario of Coal Science, *Fuel* **79**, 461 (2000).
[2] International Energy Outlook (2008). http://www.eia.doe.gov/oiaf/ieo/coal.html
[3] Clean Air Mercury Rule. www.epa.gov/air/mercuryrule
[4] J.D. Monnell, R.D. Vidic, D. Gang, A. Karash and E.J. Granite, in *Recent Advances in Trace Metal Capture Using Micro and Nano-Scale Sorbents*, Proceedings of the 23rd Pittsburgh Coal Conference, Pittsburgh, PA, 2006.
[5] E.J. Granite, H.W. Pennline and R.A. Hargis, Novel Sorbents for Mercury Removal from Flue Gas, *Ind. Eng. Chem. Res.* **39**, 1020 (2000).
[6] B. Ghorishi and B.K. Gullett, Sorption of Mercury Species by Activated Carbons and Calcium-Based Sorbents: Effect of Temperature, Mercury Concentration and Acid Bases, *Waste Mgmt. Res.* **16**, 582 (1998).
[7] A.P. Jones, J.W. Hoffmann, D.N. Smith, J. Thomas, I. Feeley and J.T. Murphy, *DOE/NETL's phase II mercury control technology field testing program, research and development solutions,* LLC, U.S. Department of Energy, National Energy Technology Laboratory, U.S. Department of Energy, Office of Fossil Energy (2006).
[8] S.V. Krishnan, B.K. Gullett and W. Jozewicz, Sorption of Elemental Mercury by Activated Carbons, *Environ. Sci. Technol.* **28**, 1506 (1994).
[9] R.D. Vidic and D.P. Siler, Vapor-Phase Elemental Mercury Adsorption by activated Carbon Impregnated with Chloride and Chelating Agents, *Carbon* **39**, 3 (2001).
[10] B. Padak, M. Brunetti, A. Lewis and J. Wilcox, Mercury Binding on Activated Carbon, *Environ. Prog.* **25**, 319 (2006).
[11] D. Styris, L.J. Prell, D.A. Redfield, J.A. Holcombe, D.A. Bass and V. Majidi, Mechanisms of Selenium Vaporization with Palladium Modifiers Using Electrothermal Atomization and Mass Spectrometric Detection, *Anal. Chem.* **63**, 508 (1991); J.P. Matousek, R. Iavetz, K.J. Powell and H. Louie, Mechanistic Studies on the Trapping and Desorption of Volatile Hydrides and Mercury for their Determination by Electrothermal Vaporization-Inductively-Coupled Plasma Mass Spectrometry, *Spectrochim. Acta B* **57**, 147 (2002); B. Docekal, J. Dedina and V. Krivan, Radiotracer Investigation of Hydride Trapping Efficiency within a Graphite Furnace, *Spectrochim. Acta B* **52**, 787 (1997).

[12] S.V. Krishnan, B.K. Gullett and W. Jozewicz, Sorption of Elemental Mercury by Activated Carbons, *Environ. Sci. Technol.* **28**, 1506 (1994).
[13] S. Poulston, E.J. Granite, H.W. Pennline, C.R. Myers, D.C. Stanko, H. Hamilton, L. Rowsell, T. Ilkenhans and W. Chu, Metal Sorbents for High Temperature Mercury Capture from Flue Gas, *Fuel* **86**, 2201 (2007).
[14] E.J. Granite, C.R. Myers, W.P. King, D.C. Stanko, H.W. Pennline and W. Henry, Sorbents for Mercury Capture from Fuel Gas with Application to Gasification Systems, *Ind. Eng. Chem. Res.* **45**, 4844 (2006).
[15] J.A. Steckel, Density Functional Theory Study of Mercury Adsorption on Metal Surfaces, *Phys. Rev. B.* **77**, 115412 (2008).
[16] A.L. Neme, W.C. Wagner and W. O'Brien, Effects of Palladium Addition on Emission of Mercury Vapor from Dental Amalgam, *Dent. Mater.* **15**, 382 (1999); M. Koike, J.L. Ferracane, J.D. Adey, H. Fujii and T. Okabe, Initial Mercury Evaporation from Experimental Ag-Sn-Cu Amalgams Containing Pg, *Biomaterials* **25**, 3147 (2004); K.I. Chen, C.P. Ju and J.H. Chern Lin, Effect of Particle Configuration on Structure and Properties of Dispersed Pd-Containing Dental Amalgam, *Biomaterials* **20**, 1851 (1999).
[17] D.R. Alfonsa, A.V. Cugini and D.S. Sholl, Density Function Studies of Sulfur Binding on Pd, Cu and Ag and Their Alloys, *Surf. Sci.* **546**, 12 (2003).
[18] G. Kresse and J. Furthmuller, Efficiency of Ab-Inition Total Energy Calculations for Metals and Semiconductors Using a Plane-Wave Basis Set, *Comput. Mater. Sci.* **6**, 15 (1996); G. Kresse and J. Hafner, Ab initio Molecular Dynamics for Open-Shell Transition Metals, *Phys. Rev. B* **48**, 13115 (1993); G. Kresse and J. Hafner, Ab initio Molecular-Dynamics Simulation of the Liquid-Metal-Amorphous-Semiconductor in Germanium, *Phys. Rev. B* **49**, 14251 (1994).
[19] D. Vanderbilt, Soft Self-Consistent Pseudopotentials in a Generalized Eigenvalue Formalism, *Phys. Rev. B.* **41**, 7892 (1990); G. Kresse and J. Hafner, Norm-Conserving and Ultrasoft Pseudopotentials for First-Row and Transition Elements, *J. Phys. Condens. Matter.* **6**, 8245 (1994).
[20] J.P. Perdew and Y. Wang, Accurate and Simple Analytic Representation of the Electron-Gas Correlation Energy, *Phys. Rev. B.* **45**, 13244 (1992).
[21] P. Schwerdtfeger, R. Wesendrup, G.E. Moyano, A.J. Sadlej, J. Greif and F. Hensel, The Potential Energy Curve and Dipole Polarizability Tensor of Mercury Dimer, *J. Chem. Phys.* **115**, 7401 (2001); G. Kresse and J. Hafner, Ab Initio Simulation of the Metal/Nonmetal Transition in Expanded Fluid Mercury, *Phys. Rev. B.* **55**, 7539 (1997); N. Gaston and P. Schwerdtfeger, From the van der Waals Dimer to the Solid State of Mercury with Relativistic Ab Initio and Density Functional Theory, *Phys. Rev. B.* **74**, 024105 (2006).
[22] J. Koperski, B. Atkinson and L. Krause, The $0_u^+(6^3P_1) \leftarrow X0_g^+$ Spectrum of Hg_2 Excited in a Supersonic Jet, *Chem. Phys. Lett.* **219**, 161 (1994).
[23] M. Methfessel and A.T. Paxton, High-Precision Sampling for Brillouin-Zone Integration in Metals, *Phys. Rev. B.* **40**, 3616 (1989).
[24] H.J. Monkhorst and J.D. Pack, Special Points for Brillouin-Zone Integrations, *Phys. Rev. B.* **13**, 5188 (1976).
[25] W.B. Pearson, *A Handbook of Lattice Spacing and Structure of Metal and Alloys*, Vol 2, (Pergamon Press, NY, USA, 1967).
[26] T.C. Leung, C.L. Kao, W.S. Su, Y.J. Feng and C.T. Chan, Relationship Between Surface Dipole, Work Function and Charge Transfer: Some Exceptions to an Established Rule, *Phys. Rev. B.* **68**, 195408 (2003).